

Hydrogen-Bonded Networks in Acetone-Alcohol Binary Mixture: Molecular Dynamics Study

Abdulkareem U (✉ akareem28@gmail.com)

Central University of Tamil Nadu <https://orcid.org/0000-0003-1753-751X>

Thejus R Kartha

International School of Engineering (INSOFE)

V Madhurima

Central University of Tamil Nadu

Research Article

Keywords: Hydrogen bonds, Molecular Dynamics Simulation, Binary Mixtures, Graph theory, Hydrogen bond network

Posted Date: March 31st, 2022

DOI: <https://doi.org/10.21203/rs.3.rs-1456979/v1>

License: © ⓘ This work is licensed under a Creative Commons Attribution 4.0 International License. [Read Full License](#)

Abstract

Our previous studies on various hydrogen-bonded binary systems have shown anomalous physico-chemical properties at lower (10–30%) volume concentrations of either one or both of the components [1]. In order to have a better understanding of this phenomenon, a systematic molecular dynamics study of binary mixtures of acetone with 8 primary alcohols (R-OH, with R = 1 to 8) was undertaken. The radial distribution function results indicate that the hydrogen bond distribution among alcohols in R=(1, 2) increases as the concentration of acetone increases, indicating the hydrogen bond networks are not disrupted by acetone, unlike that of higher alcohols. It is also seen, from the hydrogen bond statistics, that the number of acetone-alcohol hydrogen bonds are predominant for R= (3, 4, 6) and the hydrogen bonds between alcohols for the rest, suggesting R= (3, 4, 6) are attractive to acetone compared to other alcohols. The hydrogen bond networks are visualized using the graph-theoretical approach to get a clearer picture of their hydrogen-bonding network. With an increase in acetone concentration, the average number of degrees of association decreases for all systems, showing an overall decrease in hydrogen bond multimers structures.

Introduction

Hydrogen bonds (HBs) are responsible for the unusual properties of water [2] and play a crucial role in many other biological systems [3], for example in binding the two strands of DNA together [4], in explaining how protein molecules fold and in the assembling of micelles [5–6]. Despite their role in many natural phenomena, HBs find application in many modern techniques such as nanofluidics [7], self-assembly of droplets [8] and drug designing [9].

To gather a deeper understanding of the same, propose using prototypes that help focus attention to HBs that occur in many chemical or biological systems. The interactions between the carbonyl group in acetone and the hydroxyl group of alcohols act as a prototype for HBs in amino acids. Also, the study of acetone-alcohol binary mixtures will provide information about the structural changes of the solvent as the concentration changes which is useful in many medical and industrial applications. The binary mixtures of acetone with different alcohols show varying characteristics. It is interesting to note that acetone forms an azeotrope with methanol but not with any other alcohol.

Molecular Dynamics (MD) simulations are used widely to study the structural and dynamical properties of multicomponent liquid mixtures [10–13]. However, not many studies have been conducted on acetone-alcohol binary mixtures, especially for higher alcohols. Acetone-methanol and acetone-water binary mixture MD simulations were carried out by Perara *et al.*, [14] to study the micro-heterogeneities in the mixture and concluded that methanol behaves differently in water and acetone, with the microstructure of methanol being better preserved in acetone than in water. MD simulation study with acetone as a common solvent in non-polar liquids (benzene, pentane, and carbon tetrachloride) and methanol was undertaken by Pozar *et al.*, [15] to study the structuring in mixtures. The structural and energy distribution of the non-polar solvents in acetone was seen to be similar and there was a weak local ordering of the acetone molecules. On the other hand, in the methanol-acetone mixture, complex structuring is governed by methanol molecules.

In this paper, the binary mixture of acetone with alcohols (R-OH, with R = 1–8: R = 1 (methanol), R = 2 (ethanol), R = 3 (1-propanol), R = 4 (1-butanol), R = 5 (1-pentanol), R = 6 (1-hexanol), R = 7 (1-heptanol), and R = 8 (1-octanol)) is studied using MD simulations to examine their structure and HB characteristics. The effect of alkyl chain length and the solvent concentration on HB characteristics and dynamics are studied. The results are analyzed with reference to radial distribution function, HB statistics, and Graph Theoretical Approach (GTA) [16].

Methodology

Simulation Details:

Classical molecular dynamics (MD) simulations, using OPLS/AA force field [17–18] with GROMACS software [19–26] were carried out for a total time aggregate of 2088 ns. The binary mixtures of acetone with alcohols (R = 1–8) are prepared with 1000 molecules in different number concentrations of ratio 1:9 to 9:1 along with their respective pure forms. The initial coordinates were generated using Packmol software [27]. The generated input coordinates of all the systems were energy-minimized using the steepest descent algorithm [28]. The energy minimized system is then annealed from 498 K to 298.15 K reducing the temperature by 20 K every 2 ps, which is then equilibrated at isothermal-isobaric (NPT) and canonical (NVT) ensembles for 5 ns each using the Berendsen barostat [29] and the V-rescale thermostat [30], respectively. The equilibrated systems were then used to run MD production for 25 ns in a microcanonical (NVE) ensemble, with coordinates and velocities saved at an interval of 1 ps. Periodic boundary conditions were applied to simulate the system to a macroscopic level. The simulation box was visualized using VMD [31]. As an example, the simulated boxes of all mixtures at 50% concentration of acetone are shown in Fig. 1. The density of the pure components is shown in Table 1. The closeness of the simulated values to their experimental counterparts is an indication of the physical validity of our simulations and is in accordance with the results prescribed in the OPLS/AA force field [17]. NetworkX module in Python is used for GTA [16]. Coordinates sampled from MD simulation at different time frames of the trajectory were used to calculate the average degree of the graphs.

Table 1
Simulated density and their experimental density [32]

Liquids	Simulated density (Kg/m ³)	Experimental density (Kg/m ³)
acetone	797.665 ± 2.43	784
methanol	773.827 ± 3.11	791
ethanol	792.807 ± 7.65	789
1-propanol	800.491 ± 2.47	799
1-butanol	796.011 ± 2.35	809
1-pentanol	815.98 ± 2.06	814
1-hexanol	810.53 ± 2.08	813
1-heptanol	824.14 ± 2.17	821
1-octanol	827.877 ± 2.08	826

Hydrogen bonds:

In Silico methods use either bond energy or bond length to determine hydrogen bonds [33–34]. Contrary to common belief [35–36], Herschal et al., recently showed that these bonds are independent of the environment [37]. In the present study, the number of HBs is calculated for all the systems using the gmh module of GROMACS, which defines HB with the inter-oxygen distance less than 0.35 nm and the O—H-O angle less than 30°.

Results And Discussion

1. Radial Distribution Function:

In an acetone-alcohol mixture, two types of strong hydrogen bonds are seen, they are

(i) O_A - HO, between the oxygen of acetone (O_A) and the hydrogen of the hydroxyl group (HO) of alcohols (Fig. 2(a)) (ii) O - HO, between the oxygen (O) and (HO) of alcohols (Fig. 2(b)).

The likelihood of finding oxygen atoms (O or O_A) in the vicinity of HO can be obtained by calculating the g(r) or the radial distribution function (RDF). g(r) gives the probability distribution of occurrence of a particle around the reference particle at a given distance r.

Figure 3(a-g) and Fig. 4(a-g) represent g(r) of O_A - HO and O - HO respectively. The first solvation maxima for all systems are obtained at ~ 0.19 nm, which are representative of the H-bonds formed in the system. This is in agreement with the hydrogen bond distances reported in the literature (0.15 nm to 3.0 nm) [38]. In order to quantify the extent to which the 'peak heights' vary, Δg(r) is calculated i.e., the difference between the first solvation maxima at the highest and the lowest concentrations of acetone:

$$\Delta g(r) = \text{Solvationmaximum}(90\% \text{acetone}) - \text{Solvationmaximum}(10\% \text{acetone})$$

Δg(r) is represented in Fig. 3(i) and 4(i).

g(r) of R=(1, 2)-acetone mixture:

As the concentration of acetone increases, R= (1, 2) -acetone mixtures show significant variations in the first solvation maxima in both O_A - HO and O - HO interactions (Figures (3 a,b and 4 a,b)). The g(r) values show a higher distribution of O-HO interaction than O_A-HO, suggesting that in R= (1, 2) -acetone mixtures, alcohol molecules show preferential solvation towards alcohol molecules. From Figures (3 a,b and 4 a,b), the first solvation maxima increases as the concentration of acetone increases. The Δg(r) calculated for R= (1, 2) -acetone mixture brings out the large difference in the solvation maxima reported in Figures (3(i) and 4(i)), indicating the significant change in hydrogen bonding behavior as the concentration of acetone changes. R= (1, 2) -acetone mixtures are systems that contain strong hydrogen bonding networks, and increasing the concentration of acetone does not break these networks between O - HO. The schematic representation of acetone molecules around the hydrogen bonding network of R = (1, 2) are given in Figures (5 a and b) indicating that increasing the concentration of acetone does not break the hydrogen-bonded network of R= (1, 2) and also acetone molecules form hydrogen bonding network of acetone molecules around R = (1, 2).

g(r) of R=(3, 4, 6)-acetone mixture:

As the concentration of acetone increases R= (3, 4) -acetone mixtures show no variations in the first solvation maxima in both O_A - HO and O - HO interactions (Figures (3 c,d, and 4 c,d)). The g(r) values show a similar distribution of O - HO and O_A - HO, suggesting that in R= (3, 4) -acetone mixtures, alcohol molecules

show no preferential solvation. In figures (3 c,d), the first solvation maxima decrease as the concentration of acetone increases showing the reversal in trend from R= (1,2) -acetone mixture. The $\Delta g(r)$ calculated for R= (3, 4) -acetone mixture brings out no difference in the solvation maxima. As Figures (3(i) and 4(i)) suggest, there is very little change in hydrogen bonding behavior as the concentration of acetone changes.

In R = 6 -acetone mixture, show significant variations in the first solvation maxima in both O_A - HO and O - HO interactions (Figures (3 f and 4 f). The $g(r)$ values show a similar distribution of O - HO and O_A - HO, suggesting that in R = 6 -acetone mixtures, alcohol molecules also show no preferential solvation. Figures (3 f and 4 f) shows that the first solvation maxima decrease the concentration of acetone increases. The $\Delta g(r)$ calculated for R= (6) -acetone mixture brings out the large difference in the solvation maxima reported in Figures (3(i) and 4(i)), indicating the significant change in hydrogen bonding behavior as the concentration of acetone changes. Increasing the concentration of acetone breaks the existing hydrogen bonded network of R = 6 -acetone mixture.

$g(r)$ of R=(5,7,8)-acetone mixture:

As the concentration of acetone increases R= (5) -acetone mixtures show no variations in the first solvation maxima of O_A - HO interactions (Fig. 3e) and little variation in O - HO interactions. As the concentration of acetone increases R= (7, 8) -acetone mixtures show small variations in the first solvation maxima of O_A - HO and O - HO interactions (Figs. 3(g,h). The $g(r)$ values show the higher distribution of O - HO interaction than O_A - HO interactions, suggesting that in R= (5, 7, 8) -acetone mixtures show preferential solvation towards alcohol molecules. The $\Delta g(r)$ calculated for R= (5, 7, 8) -acetone mixtures exhibit a small difference in the solvation maxima reported in Figures (3(i) and 4(i)), indicating a very little change in hydrogen bonding behavior as the concentration of acetone changes.

In summary, from the RDF and $\Delta g(r)$ information presented, it is concluded that there is an effect of the acetone concentration on the hydrogen bond network structure of R= (1, 2, 6), both of O_A - HO and O - HO interactions. R= (1, 2) are systems that contain strong hydrogen bonding networks, and increasing the concentration of acetone does not break these networks. For R = 6, increasing the concentration of acetone breaks the hydrogen bonding network. However, in R= (3, 4) and R= (5, 7, 8) systems, hydrogen bonding behavior, in general, shows little to no change as the concentration of acetone is altered. The inconsistent variation in the $g(r)$ as the alkyl chain length increases and the bunching of R=(1, 2), R= (3, 4, 6) and R=(5, 7, 8) -acetone mixture are explained using hydrogen bond statistics.

Hydrogen bond Statistics:

The average number of strong HBs calculated for O_A - HO, O - HO, and the total number of HBs for the entire concentration range in acetone-alcohol mixtures is reported in Table 2. The total number of HBs is given in Fig. 6 (a), O_A - HO and O - HO HBs are represented in Figs. 6 (b) and (c) respectively. The total number of hydrogen bonds decreases as the concentration of acetone increases. The R = (1, 2) -acetone mixtures show a larger number of hydrogen bonds compared to the other systems. R = (3, 4, 6) -acetone mixtures show a larger number of hydrogen bonds between acetone and alcohols rather than other alcohol mixtures which indicates the higher probability observed in $g(r)$ (Fig. 3). R = (3, 4, 6) -acetone mixtures have less value of $g(r)$ in Fig. 4. This indicates that compared with other alcohol mixtures, R = (3, 4, 6) alcohols are more attractive to acetone. In addition to the strong hydrogen bonds, the weak hydrogen bonds formed among acetone molecules, ie. The attraction between (O_A) and carbonyl hydrogen (H_C) is calculated and reported in Table 3 and represented graphically in Fig. 6 (d). The weak hydrogen bonds decrease for all concentrations of acetone as the alkyl chain of alcohol increases. R = 1 -acetone mixture has the highest number of weak hydrogen bonds. The hydrogen bond density per nm^3 is calculated and reported in Table 4 and represented in Fig. 6 (e). The R = 1 -acetone mixture has a large number density, the number density decreases as the alkyl chain length increases. The clear picture of the hydrogen bond network formed is analyzed using the GTA below.

Table 2
hydrogen bonds vs concentration of acetone for R= (1-8):

Acetone (%)	R = 1			R = 2			R = 3			R = 4			R = 5			R = 6			R = 7
	O _A	O	Total	O _A															
	-HO	-HO		-HO	-HO		-HO	-HO		-HO	-HO		-HO	-HO		-HO	-HO		-HO
10	50	760	810	47	765	812	64	600	664	64	607	671	39	658	697	63	596	659	36
20	90	627	716	84	634	718	113	479	592	115	485	600	71	543	614	112	477	590	66
30	118	505	623	111	513	624	149	370	519	151	376	527	96	437	533	149	371	520	89
40	137	394	530	130	401	531	170	276	446	173	280	453	114	339	453	170	278	448	107
50	145	293	438	139	300	439	178	194	372	181	197	378	123	251	374	179	196	375	117
60	144	203	348	140	208	348	172	125	297	175	127	303	124	171	295	174	128	302	119
70	132	125	258	129	129	258	151	72	223	155	73	228	115	104	219	154	73	227	111
80	107	62	170	105	64	170	116	32	149	119	33	152	93	51	143	119	33	152	91
90	66	18	83	64	19	83	66	8	74	68	8	76	56	14	70	68	8	77	56

Table 3
Number of hydrogen bonds between acetone molecules vs concentration of acetone

Concentration (%)	Number of Hydrogen bonds							
	R = 1	R = 2	R = 3	R = 4	R = 5	R = 6	R = 7	R = 8
10%	84	70	52	47	47	40	43	43
20%	311	266	209	190	189	164	172	169
30%	650	575	468	430	428	376	393	377
50%	1599	1479	1299	1221	1203	1102	1102	1067
60%	2185	2054	1871	2978	1745	1636	1615	1575
70%	2836	2715	2545	2451	2404	2297	2263	2209
80%	3558	3458	3329	3245	3195	3102	3058	3000
90%	4352	4290	4224	4170	4127	4070	4032	3990

Table 4
hydrogen bonds density per nm³ versus concentration of acetone (%)

Concentration (%)	Number of Hydrogen bonds							
	R = 1	R = 2	R = 3	R = 4	R = 5	R = 6	R = 7	R = 8
10%	10.9	8.2	5.3	4.4	4	3.3	3.1	2.8
20%	9	7.1	4.7	4	3.7	3.1	2.9	2.6
30%	7.4	6	4.1	3.6	3.3	2.8	2.6	2.4
40%	5.9	4.9	3.6	3.2	2.9	2.6	2.4	2.2
50%	4.6	4	2.9	2.7	2.5	2.3	2.1	1.9
60%	3.5	3.1	2.4	2.3	2	1.9	1.8	1.6
70%	2.4	2.3	1.8	1.7	1.6	1.5	1.4	1.3
80%	1.5	1.5	1.2	1.2	1.1	1.1	1	0.9
90%	0.7	0.7	0.6	0.6	0.5	0.6	0.5	0.5

Graph Theoretical Analysis:

To visualize and study the hydrogen bonding network in this system, graph theory was used on the results of MD simulations. All hydrogen-bonded structures are mapped in a two-dimensional representation using GTA for $R = (1 \text{ to } 8)$ with acetone at all concentrations. Oxygen and hydrogen atoms in the systems are considered as nodes and an edge is drawn between H-bonded atoms to illustrate the connection. A distance criterion of 0.15 to 0.25 nm between the acceptor oxygen and the donor hydrogen atoms were used to define the hydrogen bonds. This cutoff has been chosen from the RDF calculations which show the first solvation shell to exist in the 0.15–0.25 nm range. The graph theoretical representation of H-bonded networks of 10% $R = 6$ -acetone mixture is given in Fig. 7(a). The snapshot of the selected HB structures are marked to the network graphs and shown in Fig. 7 (b - f). The two-dimensional representation of $R = (1, 4, 8)$ -acetone mixtures are shown in Figures (8, 9 and 10). The ratio of the number of edges divided by the number of nodes (i.e average degree) for O_A - HO and O - HO interactions are plotted in Figs. 10 (a) and (b) respectively. It is seen from Fig. 10 (a) that the average degrees show no variations as the alkyl chain length of the alcohol increases along with the change in concentration of acetone. This is because the HB structures of acetone with alcohol are mostly dimers which is evident from the O_A - HO network structures in Figs. 8, 9, and 10. Figure 10 (b) shows that the average degree decreases as the concentration of acetone increases. The bunching of (i) $R = (1, 2)$ -acetone mixtures, (ii) $R = (3, 4, 6)$ -acetone mixtures, and (iii) $R = (5, 7, 8)$ -acetone mixtures are seen. This bunching is also observed in hydrogen bond statistics. $R = (1, 2)$ -acetone mixtures have the highest number of average degrees indicating more HB networks are formed between alcohols. $R = (3, 5, 6)$ -acetone mixtures have the lowest average degrees. The number of HB multimers decreases in increasing the concentration of acetone for all alcohols.

Conclusion

Hydrogen bonding interactions play a significant role in dictating the properties of binary liquid mixtures, which find applications in many fields such as surface physics, biomolecular interactions, etc. To understand this at a molecular level, as prototypes for O-H hydrogen bonding, binary mixtures of acetone with primary alcohols (R-OH) of $R = (1 \text{ to } 8)$ were studied using classical molecular dynamics. The structural properties of HB networks were studied using radial distribution function, HB statistics, and graph-theoretical approach (GTA). The variation of hydrogen-bond network structures are reported for (a) various acetone-alcohol mixtures ($R = 1-8$ for alcohols) with a change in the concentration and (b) the dependence of alkyl chain length in the microscopic structure of the hydrogen bonds in the acetone-alcohol binary liquids. Clearly, bunching in the HB characteristics are seen among $R = (1, 2)$, $R = (3, 4, 6)$ and $R = (5, 7, 8)$ -acetone mixtures. In $R = (1, 2)$, the results from RDF and GTA show the hydrogen-bonded network does not break while increasing the concentration of acetone, whereas among other alcohols the HB network is broken by the acetone molecules as the concentration of acetone increases. Also, $R = (1, 2)$ -acetone mixtures exhibit preferential solvation to alcohols which is evident from RDF results. In $R = (3, 4, 6)$ -acetone mixture shows no preferential solvation at all concentrations and also compared with other alcohol mixtures $R = (3, 4, 6)$ are more attractive to acetone which is evident from HB statistics and GTA results. In $R = (5, 7, 8)$ -acetone mixtures, preferential solvation towards alcohols molecules are seen. The hydrogen bond number density decreases as the alkyl chain length increases. Average degrees calculated using GTA show that hydrogen-bonded interactions with acetone are mostly dimers, and the HB networks reduce as the concentration of acetone increases.

Declarations

Acknowledgements:

The authors acknowledge the use of the Inter-University Center for Astronomy and Astrophysics (IUCAA) server to run the MD simulations. AU acknowledges the Central University of Tamil Nadu, India for providing university fellowship.

Funding:

The authors declare that no funds, grants, or other support were received during the preparation of this manuscript.

Competing Interests:

The authors have no relevant financial or non-financial interests to disclose.

Author Contributions:

AU and TRK performed all the simulations, all the authors were involved in the analysis of the results and contributed equally to the consolidation of results, writing and editing of the manuscript.

Data Availability:

The datasets generated during and/or analyzed during the current study are available from the corresponding author on reasonable request.

References

1. Nilavarasi K, Kartha TR, Madhurima V (Jan. 2018) Evidence of anomalous behavior of intermolecular interactions at low concentration of methanol in ethanol-methanol binary system. *Spectrochim Acta A Mol Biomol Spectrosc* 188:301–310. doi: 10.1016/j.saa.2017.07.015
2. Demontis P, Masia M, Suffritti GB (Apr. 2014) Peculiar Structure of Water in Slightly Superhydrated Vermiculite Clay Studied by Car–Parrinello Molecular Dynamics Simulations. *J Phys Chem C* 118(15):7923–7931. doi: 10.1021/jp409723x
3. Daniel Głowacki E, Irimia-Vladu M, Bauer S, Serdar Sariciftci N (2013) Hydrogen-bonds in molecular solids – from biological systems to organic electronics. *J Mater Chem B* 1(31):3742–3753. doi: 10.1039/C3TB20193G
4. Pardo L, Campillo M, Bosch D, Pastor N, Weinstein H (2000) “Binding Mechanisms of TATA Box-Binding Proteins: DNA Kinking is Stabilized by Specific Hydrogen Bonds,” *Biophys. J.*, vol. 78, no. 4, pp. 1988–1996, Apr. doi: 10.1016/S0006-3495(00)76746-4
5. Kim B-S, Park SW, Hammond PT (2008) “Hydrogen-Bonding Layer-by-Layer-Assembled Biodegradable Polymeric Micelles as Drug Delivery Vehicles from Surfaces,” *ACS Nano*, vol. 2, no. 2, pp. 386–392, Feb. doi: 10.1021/nn700408z
6. Heinzemann G, Figueiredo W, Girardi M (Oct. 2012) Micellar dynamics and water–water hydrogen-bonding from temperature-jump Monte Carlo simulations. *Chem Phys Lett* 550:83–87. doi: 10.1016/j.cplett.2012.09.011
7. Joly L, Tocci G, Merabia S, Michaelides A (Apr. 2016) Strong Coupling between Nanofluidic Transport and Interfacial Chemistry: How Defect Reactivity Controls Liquid–Solid Friction through Hydrogen Bonding. *J Phys Chem Lett* 7(7):1381–1386. doi: 10.1021/acs.jpcl.6b00280
8. Nilavarasi K, Madhurima V (Jul. 2018) Controlling breath figure patterns on PDMS by concentration variation of ethanol-methanol binary vapors. *Eur Phys J E* 41:82. doi: 10.1140/epje/i2018-11691-x
9. Hao M-H (May 2006) Theoretical Calculation of Hydrogen-Bonding Strength for Drug Molecules. *J Chem Theory Comput* 2(3):863–872. doi: 10.1021/ct0600262
10. Essafri I, Ghoufi A (Jun. 2019) Microstructure of nonideal methanol binary liquid mixtures. *Phys Rev E* 99(6):062607. doi: 10.1103/PhysRevE.99.062607
11. Bakó I, Megyes T, Bálint S, Grósz T, Chihai V (2008) “Water–methanol mixtures: topology of hydrogen bonded network,” *Phys. Chem. Chem. Phys.*, vol. 10, no. 32, pp. 5004–5011, Aug. doi: 10.1039/B808326F
12. Zhang X et al (2021) “Using Acetone/Water Binary Solvent to Enhance the Stability and Bioavailability of Spray Dried Enzalutamide/HPMC-AS Solid Dispersions,” *J. Pharm. Sci.*, vol. 110, no. 3, pp. 1160–1171, doi: 10.1016/j.xphs.2020.10.010
13. Koch K, Górak A (Aug. 2014) Pervaporation of binary and ternary mixtures of acetone, isopropyl alcohol and water using polymeric membranes: Experimental characterisation and modelling. *Chem Eng Sci* 115:95–114. doi: 10.1016/j.ces.2014.02.009
14. Perera A, Zoranić L, Sokolić F, Mazighi R (Feb. 2011) A comparative Molecular Dynamics study of water–methanol and acetone–methanol mixtures. *J Mol Liq* 159(1):52–59. doi: 10.1016/j.molliq.2010.05.006
15. Požar M, Zoranić L (2020) “The structuring in mixtures with acetone as the common solvent,” *Phys. Chem. Liq.*, vol. 58, no. 2, pp. 184–201, Mar. doi: 10.1080/00319104.2018.1564305
16. Hagberg AA, Schult DA, Swart PJ (2008) “Exploring Network Structure, Dynamics, and Function using NetworkX,” in *Proceedings of the 7th Python in Science Conference*, Pasadena, CA USA, pp. 11–15. Accessed: Jan. 17, 2022. [Online]. Available: http://conference.scipy.org/proceedings/SciPy2008/paper_2/
17. Dodda LS, Cabeza de Vaca I, Tirado-Rives J, Jorgensen WL (Jul. 2017) LigParGen web server: an automatic OPLS-AA parameter generator for organic ligands. *Nucleic Acids Res* 45:W331–W336. no. W1 doi: 10.1093/nar/gkx312
18. “Development and Testing of the OPLS All-Atom Force Field on Conformational Energetics (1996) Properties of Organic Liquids. *J Am Chem Soc* 118(45):11225–11236. doi: 10.1021/ja9621760
19. Abraham MJ, “GROMACS et al (2015) High performance molecular simulations through multi-level parallelism from laptops to supercomputers. *SoftwareX* 1–2 19–25, Sep. doi: 10.1016/j.softx.2015.06.001
20. Bekker H et al (1993) “GROMACS - A PARALLEL COMPUTER FOR MOLECULAR-DYNAMICS SIMULATIONS,” in *PHYSICS COMPUTING '92*, pp. 252–256. Accessed: Jun. 22, 2021. [Online]. Available: <https://research.rug.nl/en/publications/gromacs-a-parallel-computer-for-molecular-dynamics-simulations>
21. Berendsen HJC, van der Spoel D, van Drunen R (Sep. 1995) GROMACS: A message-passing parallel molecular dynamics implementation. *Comput Phys Commun* 91:1–3. doi: 10.1016/0010-4655(95)00042-E
22. Hess B, Kutzner C, van der Spoel D, Lindahl E (2008) “GROMACS 4: Algorithms for Highly Efficient, Load-Balanced, and Scalable Molecular Simulation,” *J. Chem. Theory Comput.*, vol. 4, no. 3, pp. 435–447, Mar. doi: 10.1021/ct700301q

23. Kutzner C, Páll S, Fechner M, Esztermann A, de Groot BL, Grubmüller H (Oct. 2015) Best bang for your buck: GPU nodes for GROMACS biomolecular simulations. *J Comput Chem* 36(26):1990–2008. doi: 10.1002/jcc.24030
24. Kutzner C, Páll S, Fechner M, Esztermann A, Groot BL, Grubmüller H (2019) “More bang for your buck: Improved use of GPU nodes for GROMACS 2018,” *J. Comput. Chem.*, vol. 40, no. 27, pp. 2418–2431, Oct. doi: 10.1002/jcc.26011
25. Lindahl E, Hess B, van der Spoel D (2001) “GROMACS 3.0: a package for molecular simulation and trajectory analysis,” *J. Mol. Model.*, vol. 7, no. 8, pp. 306–317, Aug. doi: 10.1007/s008940100045
26. Van Der Spoel D, Lindahl E, Hess B, Groenhof G, Mark AE, Berendsen HJC (2005) “GROMACS: Fast, flexible, and free,” *J. Comput. Chem.*, vol. 26, no. 16, pp. 1701–1718, Dec. doi: 10.1002/jcc.20291
27. Martínez L, Andrade EGBR, Martínez JM (2009) Packmol: A package for building initial configurations for molecular dynamics simulations. *J Comput Chem* 30(13):2157–2164
28. Abraham MJ, Lindahl E, Lindahl E, Hess B GROMACS, and development team, “GROMACS User Manual version 5.0.6.” [Online]. Available: www.gromacs.org
29. Berendsen HJC, Postma JPM, van Gunsteren WF, DiNola A, Haak JR “Molecular dynamics with coupling to an external bath,” *J Chem Phys*, vol. 81, no. 8, doi: 10.1063/1.448118
30. Bussi G, Donadio D, Parrinello M (Jan. 2007) Canonical sampling through velocity rescaling. *J Chem Phys* 126(1):014101. doi: 10.1063/1.2408420
31. Humphrey W, Dalke A, Schulten K (1996) Visual molecular dynamics. *J Mol Graph* 14(1):33–38. doi: [https://doi.org/10.1016/0263-7855\(96\)00018-5](https://doi.org/10.1016/0263-7855(96)00018-5)
32. Lide D (2010) *CRC Handbook of Chemistry and Physics*, 90th ed.
33. Stumpe MC, Grubmüller H (2007) “Aqueous Urea Solutions: Structure, Energetics, and Urea Aggregation,” *J. Phys. Chem. B*, vol. 111, no. 22, pp. 6220–6228, Jun. doi: 10.1021/jp066474n
34. Luzar, Chandler “Effect of Environment on Hydrogen Bond Dynamics in Liquid Water,” *Am. Phys. Soc.*, vol. 76, no. 6, pp.928–931, doi: 10.1103/PhysRevLett.76.928
35. Gao J, Bosco DA, Powers ET, Kelly JW (2009) “Localized thermodynamic coupling between hydrogen bonding and microenvironment polarity substantially stabilizes proteins,” *Nat. Struct. Mol. Biol.*, vol. 16, no. 7, pp. 684–690, Jul. doi: 10.1038/nsmb.1610
36. Gerlt JA, Kreevoy MM, Cleland WW, Frey PA (Apr. 1997) Understanding enzymic catalysis: the importance of short, strong hydrogen bonds. *Chem Biol* 4(4):259–267. doi: 10.1016/S1074-5521(97)90069-7
37. Herschlag D, Pinney MM (Jun. 2018) Hydrogen Bonds: Simple after All? *Biochemistry* 57(24):3338–3352. doi: 10.1021/acs.biochem.8b00217
38. “Chapter 1 (2020) Hydrogen Bond – Definitions, Criteria of Existence and Various Types. ” in *Theoretical and Computational Chemistry Series*. Royal Society of Chemistry, Cambridge, pp 1–40. doi: 10.1039/9781839160400-00001.

Figures

Figure 1

Simulated boxes of 50% concentration of acetone in (a) R=1, (b) R=2, (c) R=3, (d) R=4, (e) R=5, (f) R=6, (g) R=7 and (h) R=8. Acetone is represented in red color and the second color indicates the respective alcohols.

Figure 2

Hydrogen bonds formed (a) between the oxygen of acetone (O_A) and the hydrogen of the hydroxyl group (HO) of alcohols and (b) among the oxygen (O) and (HO) of alcohols

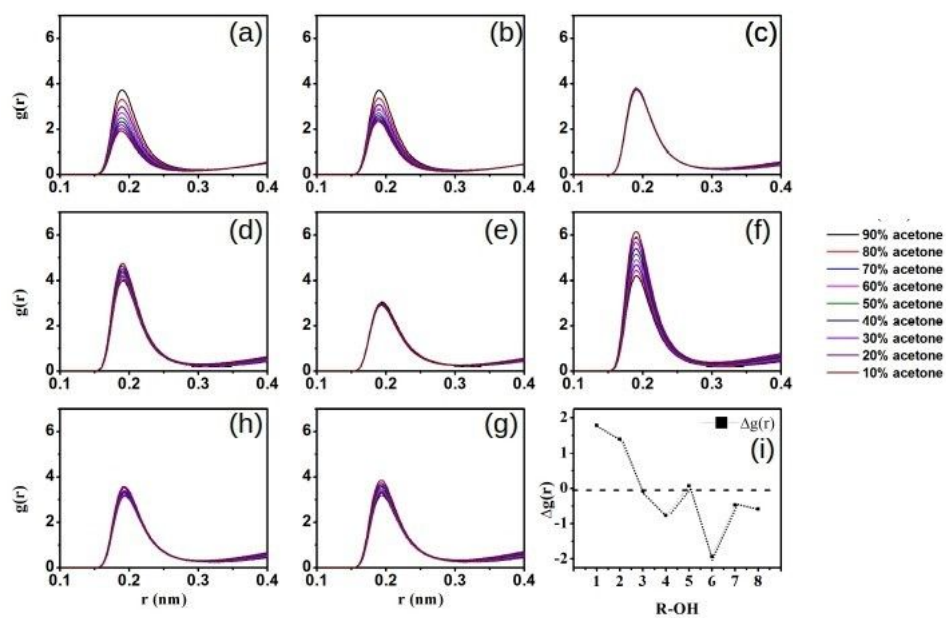


Figure 3

$g(r)$ of $O_A - HO$: (a) R-1 (b) R-2, (c) R-3, (d) R-4, (e) R-5, (f) R-6, (g) R-7, (h) R-8.

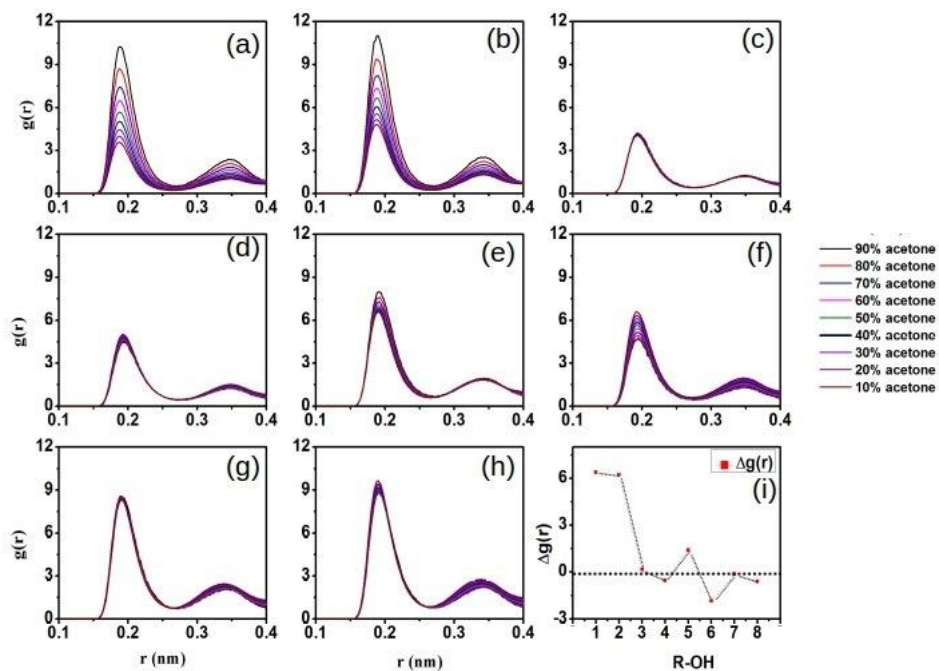


Figure 4

$g(r)$ of $O - HO$: (a) R-1 (b) R-2, (c) R-3, (d) R-4, (e) R-5, (f) R-6, (g) R-7, (h) R-8.

Figure 5

(a) Acetone molecules around methanol trimers, (b) Acetone molecules around ethanol trimers (snapshot taken from 80% concentration of acetone)

Figure 6

Average number of (a) total hydrogen bonds, (b) (O_A -HO) HBs, (c) (O-HO) HBs, (d) (O_A - H_C) HBs, and (e) HBs density versus concentration of acetone (%)

Figure 7

Network graphs and molecular structures of the HB networks in the 10% concentration of acetone in R=6 system: (a) Network graph (alcohol-red, acetone-green), (b-c) Dimers, (d) Trimer, (e) pentamer and (f) tetramer: HB structures are marked to their corresponding network in (a).

Figure 8

Two-dimensional HB network graphs of R=1 -acetone mixture at 10%, 30%, 60% and 90% concentration of acetone

Figure 9

Two-dimensional HB network graphs of R=4 -acetone mixture at 10%, 30%, 60% and 90% concentration of acetone

Figure 10

Two-dimensional HB network graphs of R=8 -acetone mixture at 10%, 30%, 60% and 90% concentration of acetone

Figure 11

Average degrees of (a) O_A - HO interaction and (b) O - HO interaction with respect to the concentration of acetone (%).